JOURNAL OF SOLID STATE CHEMISTRY 106, 164–173 (1993)

A Study of Superionic $CsHSO_4$ and $Cs_{1-x}Li_xHSO_4$ by Vibrational Spectroscopy and X-Ray Diffraction

VIJAY VARMA, N. RANGAVITTAL, AND C. N. R. RAO*

Solid State and Structural Chemistry Unit and CSIR Centre of Excellence in Chemistry, Indian Institute of Science, Bangalore 560012, India

Received December 4, 1992; accepted December 23, 1992

IN HONOR OF SIR JOHN MEURIG THOMAS ON HIS 60TH BIRTHDAY

Infrared and Raman spectroscopic studies of $CsHSO_4$ suggest the occurrence of the following phase transitions:

$$\text{IV} \underset{340\text{ K}}{\rightleftharpoons} \text{III} \underset{380\text{ K}}{\rightleftharpoons} \text{II} \underset{417\text{ K}}{\rightleftharpoons} \text{I}.$$

While the ordered phase, IV, has a monoclinic structure, the high-temperature superionic phase, I, has a tetragonal structure involving the free rotation of HSO_4^-. Phase II is close to being orthorhombic with a small monoclinic distortion. The transition to the superionic phase, I, is accompanied by the appearance of broad, structureless bands in the infrared and Raman spectra, as well as changes in the O–H stretching region due to decrease in hydrogen bonding. Accompanying the III–II transition, we observe the disappearance of the O · · · O stretching and δ(S–OH) bands and a decrease in the HSO_4^- libration frequency. Across the phase transitions, the separation between the ν(S–O) and ν(S–OH) bands shows stepwise changes. The high-temperature superionic phase essentially has sulfate-like species with a relatively short S–O bond, in contrast to the low-temperature phase, which has long and short S–O distances. Substitution of Cs by Li in $CsHSO_4$ has an effect similar to that of increasing the temperature. The vibrational spectrum of $Cs_{0.7}Li_{0.3}HSO_4$ corresponds to a state of disorder between those of phases II and I.

Introduction

Compounds of the type $MHXO_4$ (M = Rb, Cs, etc., and X = S, Se) are known to exhibit interesting phase transitions in the solid state involving rotational motions of the HXO_4 ions and in some instances the translational motion of the cations or protons as well (*1*). High-temperature phases of such solids are generally found to be superionic or plastic. A particularly interesting member of this family of solids is cesium hydrogen sulfate, $CsHSO_4$, which is reported to undergo a phase transition around 417 K to a superionic state (*2*). A phase transition has been reported at 318 K, although it is subject to some doubt (*3*). A phase transition from the room-temperature phase to an intermediate phase has been suggested to occur around 335 K associated with the transformation of the HSO_4 chains to HSO_4 dimers. Infrared and Raman spectra of $CsHSO_4$ through the phase transitions have been investigated by Pham-Thi *et al.* (*4*) and Dmitriev *et al.* (*5, 6*). These workers have discussed the changes in the spectra in terms of hydrogen bonding and structural disorder. Studies of the different phases of $CsHSO_4$ by inelastic neutron scattering and neutron diffraction have also been reported

* To whom correspondence should be addressed.

0022-4596/93 $5.00

(7–9). Besides the phase transitions at 340 K and 417 K, a transition around 380 K has been suggested to occur based on calorimetry by Baranowski *et al.* (*10*).

In spite of several investigations, there are many aspects of the occurrence and the nature of the phase transitions of $CsHSO_4$ that are not clearly understood. We have investigated the phase transitions of $CsHSO_4$ by employing infrared and Raman spectroscopy over the temperature range 300–450 K. The study has not only unravelled the nature of structural changes with increasing temperature, but has also established the occurrence of two phase transitions around 340 and 380 K, before the transition to the superionic phase at 417 K. We have studied $CsHSO_4$ by variable-temperature X-ray diffraction, to establish the structures of the different phases. We have examined the infrared and Raman spectra of $Cs_{1-x}Li_xHSO_4$ since substitution of Cs by Li is known to affect the properties substantially (*11*). The present study has shown that substitution of Cs by Li up to 30% gives rise to a room-temperature phase which has properties somewhere between those of the high-temperature superionic phase and the room-temperature phase of $CsHSO_4$.

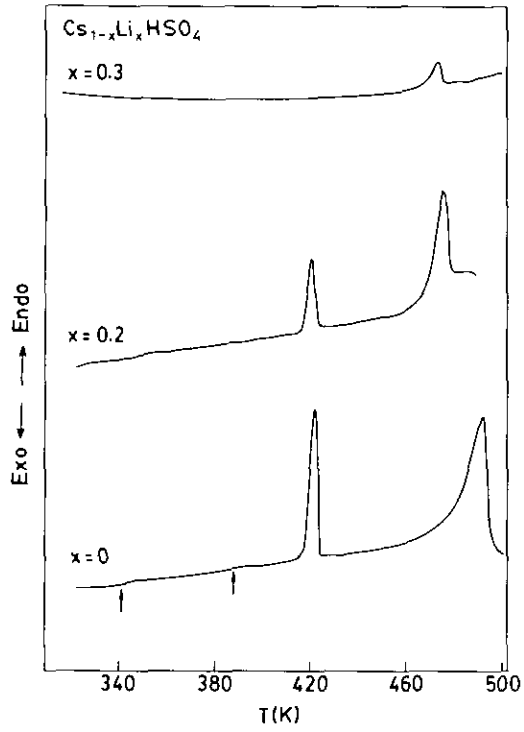

FIG. 1. Differential scanning calorimetry of $Cs_{1-x}Li_xHSO_4$.

Experimental

$CsHSO_4$ was prepared by evaporation of stoichiometric aqueous solutions of Cs_2CO_3 and H_2SO_4. $Cs_{1-x}Li_xHSO_4$ was similarly prepared by taking the required quantity of Li_2CO_3 along with Cs_2CO_3. The samples were characterized by differential scanning calorimetry (DSC) and X-ray diffraction. Differential scanning calorimetry was carried out with a Perkin–Elmer (DSC-2) instrument. We show typical DSC traces in Fig. 1. Infrared spectra were recorded with a Brüker IFS 113V FT-IR spectrometer. Spectra were recorded in KBr (3500–500 cm^{-1}) and polyethylene (300–50 cm^{-1}) matrices and with powdered sample between two CsI windows (500–300 cm^{-1}). Polyethylene melts before the occurrence of the superionic transition. A Specac variable-temperature cell and temperature controller were used for variable-temperature IR studies. Raman spectra were recorded with a Spex 1403 Laser Raman Spectrometer using the 514.5 nm line of a Spectra-Physics Argon ion laser.

High-resolution X-ray diffraction data of $CsHSO_4$ at different temperatures were obtained with a STOE automatic powder diffractometer using a Ge(111) monochromator, $CuK\alpha_1$ (λ = 1.5406 Å) radiation, and a linear PSD in the transmission mode. For the high-temperature data collection the sample was loaded in a quartz capillary and kept rotating in a graphite heating element. The temperature was measured using a EUROTHERM temperature controller. The patterns were indexed using the INDEX program of STOE and then refined using LATREF and RS PFSR PACKAGE.

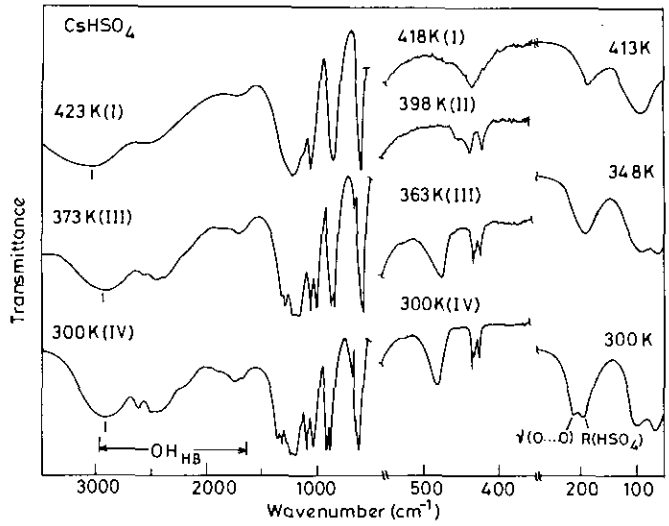

FIG. 2. Infrared spectra of the different phases of $CsHSO_4$.

Results and Discussion

Spectroscopic Study of $CsHSO_4$

In Fig. 2 we show the infrared spectra of $CsHSO_4$ at different temperatures corresponding to the different phases. The main changes in the spectra are in the O–H stretching, S–O stretching, S–OH deformation, and S–O deformation modes and in the 220–190 cm^{-1} region involving the O · · · O stretching of the hydrogen bond and the librational motion of the HSO_4^- ion. We also note changes in the translational (T′ HSO_4^-) region around 100 cm^{-1}. We see from Fig. 2 that the structure of the O–H stretching band at 300 K is typical of a moderately hydrogen-bonded system giving rise to an ABC type absorption centered around 2400 cm^{-1}, as pointed out by Pham-Thi *et al.* (9). With increase in temperature, changes occur in the structure of this band, accompanied by an increase in the ν(OH) stretching frequency in the high-temperature phase. Clearly, the strength of hydrogen bonding decreases substantially in the high-temperature phase. Accordingly, we see interesting changes in the relevant low-frequency bands as well. At 300 K there is a doublet in the infrared spectrum with maxima at 208 and 196 cm^{-1}. The band at 208 cm^{-1} disappears around 380 K, well before the transformation to the superionic state; in addition, the frequency of the 196 cm^{-1} band decreases gradually to 180 cm^{-1} at 413 K. We assign the 208 cm^{-1} band to the O · · · O stretching mode, since it would disappear in the absence of hydrogen bonding as in the high-temperature superionic phase. The 196 cm^{-1} band, in the room-temperature phase, considered to be due to the libration mode of the HSO_4^- ion, softens till nearly free rotation sets in at high temperatures. The doublet around 100 cm^{-1} at 300 K due to translation of HSO_4^- becomes a single band at 413 K. These changes show that with increasing temperature, the HSO_4^- species essentially becomes free, accompanying the decrease in hydrogen bonding. Consistent with the HSO_4^- species becoming free at high temperatures, we see interesting changes in the 420 cm^{-1} band due to the $\delta(SO_4)$ mode. This band, appearing as a triplet at 300 K, becomes a broad single band above the superionic transition temperature. The broad band around 470 cm^{-1} due to S–OH deformation disappears around 380 K, prior to the transition to the superionic phase at 417 K.

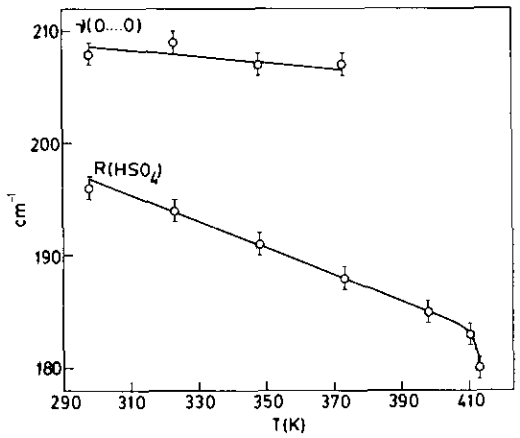

FIG. 3. Temperature variation of the infrared band frequencies due to the HSO_4^- libration and the O · · · O stretching modes.

In Fig. 3 we have shown the variation of the positions of the infrared bands at 208 and 196 cm^{-1} with temperature. We see that the 208 cm^{-1} band disappears abruptly around 380 K, while the other band undergoes a progressive shift to lower frequency, with a sharp decrease around 413 K. The total band area under the band envelope covering both the 208 and 196 cm^{-1} bands is plotted against temperature in Fig. 4a. There is a drop in intensity around 340 K and again around 380 K. The intensity of the 470 cm^{-1} band due to δ(SOH) goes to zero around 380 K, as can be seen from Fig. 4b. These changes suggest the occurrence of phase transitions around 340 and 380 K.

In Fig. 5 we show the Raman spectra of $CsHSO_4$ at different temperatures. Significant changes occur in the ν(S–O) and ν(S–OH) stretching bands appearing around 999 and 863 cm^{-1} respectively at 300 K. With increase in temperature, the frequency of the ν(S–O) mode increases while that of the ν(S–OH) mode decreases, causing the separation between the two bands to increase. The bands become broad in the superionic phase. The $\nu_3(SO_4)$ band (1050–1260 cm^{-1}) disappears around 380 K, while the $\nu_4(SO_4)$ band (570–620 cm^{-1}) loses its structure. In Fig. 6 we have plotted the changes in the frequencies of the ν(S–O) and ν(S–OH) bands with temperature. There is a sharp increase in the ν(S–O) frequency and a corresponding decrease in the ν(S–OH) frequency around 340 K and similar though smaller changes around 380 K. There are larger changes in these band frequencies around 417 K, when the material becomes superionic. In the inset of Fig. 6 we have plotted Δν(S–O/S–OH) to demonstrate the occurrence of phase transitions around 340, 380, and 417 K. The width of the ν(S–O) band also shows marked changes around 380 and 417 K. By the nature of the variations of the ν(S–O) and ν(S–OH) band frequencies, it appears that the transitions around 340 and 417 K are both first order. This is in agreement with calorimetric studies which show finite changes in latent heat at these temperatures. Baranowski *et al.* (*10*) have reported a latent heat change of 1.1 kJ mol^{-1} for a transition around 375 K. We find a somewhat vague suggestion of a

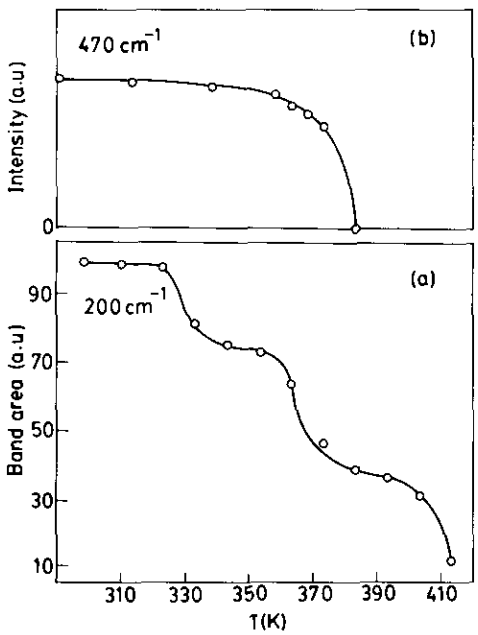

FIG. 4. Temperature dependence of the intensity of (a) the 200 cm^{-1} doublet due to ν (O · · · O) and $R(HSO_4)$ and (b) the 470 cm^{-1} (S–OH deformation) bands.

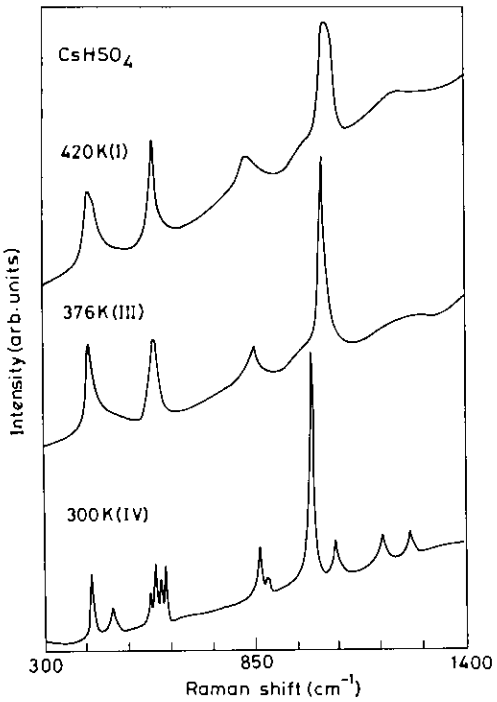

FIG. 5. Raman spectra of the different phases of $CsHSO_4$.

brational bands of phase I (Figs. 3 and 5) are clearly characteristic of such a disordered state.

X-Ray Diffraction Study of $CsHSO_4$

The room-temperature phase (IV) of $CsHSO_4$ (space group $P2_1/m$) consists of a hexagonal array of Cs^+ ions stacked along one direction with zigzag chains of hydrogen bonded HSO_4^- ions perpendicular to it (*12*). The monoclinic unit cell parameters of phase IV are $a = 7.339$, $b = 5.837$, $c = 5.517$ Å and $\beta = 101.52°$. The high-temperature superionic phase I above 417 K has the space group $I\,4_{1/amd}$ (*8*). Our infrared and Raman studies suggest the occurrence of three transitions around 340, 380, and 417 K as discussed in the previous section. We have recorded the X-ray diffraction patterns of these phases at the appropriate temperatures (Fig. 8). The diffraction pattern of the room-temperature phase (IV) is in agreement with the reported monoclinic structure. A comparison of the diffraction

phase transition around 380 K in the DSC recorded by us (see Fig. 1).

Based on the present study of temperature-dependent infrared and Raman spectra, we depict the phase transitions of $CsHSO_4$ as follows:

$$\text{IV} \underset{340\text{ K}}{\rightleftharpoons} \text{III} \underset{380\text{ K}}{\rightleftharpoons} \text{II} \underset{417\text{ K}}{\rightleftharpoons} \text{I} \underset{480\text{ K}}{\rightleftharpoons} \text{melt}.$$

We see no evidence for the 318 K transition reported by some workers. In Table I we list the major vibrational bands of the four phases of $CsHSO_4$ with assignments. In Fig. 7, we show the Raman spectra in the 900–1100 cm^{-1} region at temperatures close to the IV–III transition to demonstrate the coexistence of the two phases in the transition region. It would appear that the IV and III phases are structurally similar. Our spectroscopic results show that the phase I of $CsHSO_4$ is plastic and superionic, involving free rotation of HSO_4^- and translational disorder of protons and cations. The broad vi-

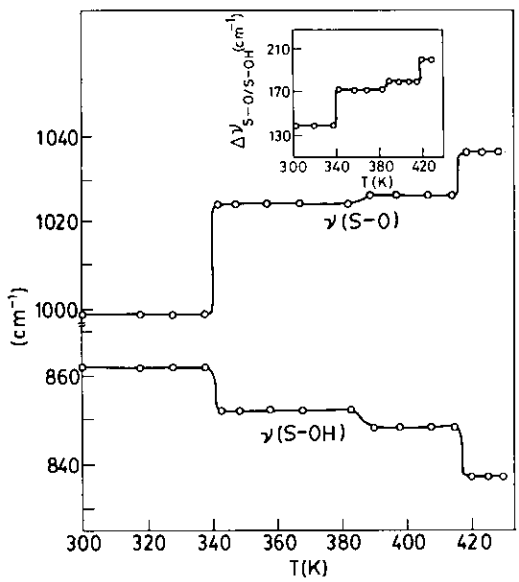

FIG. 6. Temperature dependence of ν(S–O) and ν(S–OH) Raman bands of $CsHSO_4$. Inset shows the variation of the separation between the two bands with temperature.

TABLE I

INFRARED AND RAMAN SPECTRA OF THE DIFFERENT PHASES OF $CsHSO_4$

300 K (IV)		360 K (III)		400 K (II)		423 K (I)		
IR	Raman	IR	Raman	IR	Raman	IR	Raman	Assignment
2920s,vb		2952s, b		3000s,b		3020s,b		(A)
2600 m		2590m		2500m				
2480, 2384 m		2446m		—		2504m,b		(B) O–H stretch
1745, 1659 m	a	1742, 1660 m	a	1740, 1660 m	a	1683w,b	a	(C)
1330, 1288 m		1320 w, 1289 m		1320sh, 1289w		1300sh		O–H deformation
1250s	1253m(A_g)	1218s	1214m	1218s	1214m,b	1211s,vb	1214m,b	$\nu_3(SO_4)$
1219s(A_u)	1185(A_g)	1180s		1180s		1117sh		
1180s(B_u)								
1068s		1068s	1060m	1068s	—			
1048w(A_u)	1059m(B_g)	1049w	1024s	—	1024s,b	1055s	1036s,vb	S–O stretch
1005s	999s(A_g)	1008s	991w	1005s	990w		995w	
887s	883w	884s		884s				
875w(B_u)	863m(B_g)	875w		875w	848m,b	842s	838m,vb	S–OH stretch
850s(A_u)		846s	852m	846s				
647m		647w		600sh				
613s	616m(A_g)	613m	589m	590s	589m	586s	589m,b	$\nu_4(SO_4)$
586s(A_g)	605m(B_g)	586s	—					
573s(B_u)	591m(B_g)	573s						
	575m(A_g)							
470m	477m(B_g)	470m	470m	—	—	—	—	S–OH deformation
425m(B_u)	423m(A_g)	425m		447w				
422m	423m(B_g)	422m	420m	429m	420m	430m,b	423m,vb	$\delta(SO_4)$
416m		416m		414m				
208m(B_u)	215m(B_g)	208sh	—	—	—	—	—	O · · · O stretch
196m(A_u)	—	190m		184m		170m		R HSO_4^-
100m(A_u)	a	100m	a	90m	a		a	$THSO_4^-$
70m(A_u)		70m						

Note. s—strong, m—medium, w—weak, v—very, b—broad, sh—shoulder, a—not examined.

pattern of phase III with that of phase IV shows subtle differences in the intensities of some of the peaks at higher angles, but we are able to index the pattern of III with a monoclinic cell. The absence of a significant change in crystal structure and symmetry would not be consistent with the changes observed in the vibrational spectra and latent heat. The coexistence of IV and III phases (Fig. 7), however, suggests a close similarity between the structures of the two phases. The X-ray diffraction pattern of phase II is distinctly different from those of phases III and IV. We could index the diffraction pattern to a cell with $a = 7.37$, $b = 11.14$, $c = 10.04$ Å, with a small monoclinic distortion of ($\beta = 97.19°$). The III–II transition is supposed to depend on the moisture content of the sample, the extent of grinding, and the rate of heating (*13*). In Table II, we list the unit cell parameters of phases IV, II, and I of $CsHSO_4$.

The X-ray diffraction pattern of the superionic phase (I) could be indexed in the body-centered tetragonal cell with $a = 5.714$ and $c = 14.212$ Å. The idealized model of this phase consists of two interpenetrating quasi-diamond lattices, one formed by

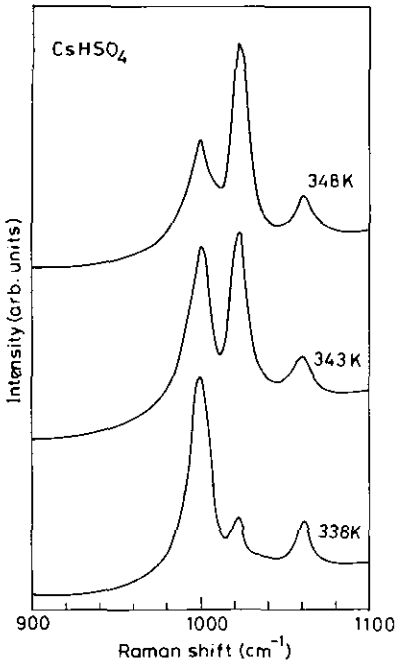

FIG. 7. ν(S–O) stretch Raman bands close to the IV–III transition of $CsHSO_4$, showing coexistence of the two phases.

the SO_4 tetrahedra and the other by the Cs^+ cations. The disordered state of protons leads to the tilting of hydrogen-bridged SO_4 tetrahedra from their ideal position (*8*). We have carried out a Rietveld profile analysis of the superionic phase based on the above model. The observed pattern has a high background and weak lines, especially at higher 2θ angles (Fig. 9). In Table III we give structural details of this phase. The S–O and Cs–O bond distances for the superionic phase I are 1.401 and 2.926 Å respectively. In the room temperature phase IV, the Cs–O bond distance ranges from 3.12 to 3.26 Å and the S–O distance ranges from 1.44 to 1.50 Å. The observation of a single S–O distance in the high-temperature phase is consistent with the presence of a sulfate-like free anion.

The structural changes from X-ray diffraction studies are consistent with our spectroscopic results, which show increasing structural disorder with increase in temperature. Thus we have monoclinic (IV) → monoclinic (III) → nearly orthorhombic (II) → tetragonal (I) transitions.

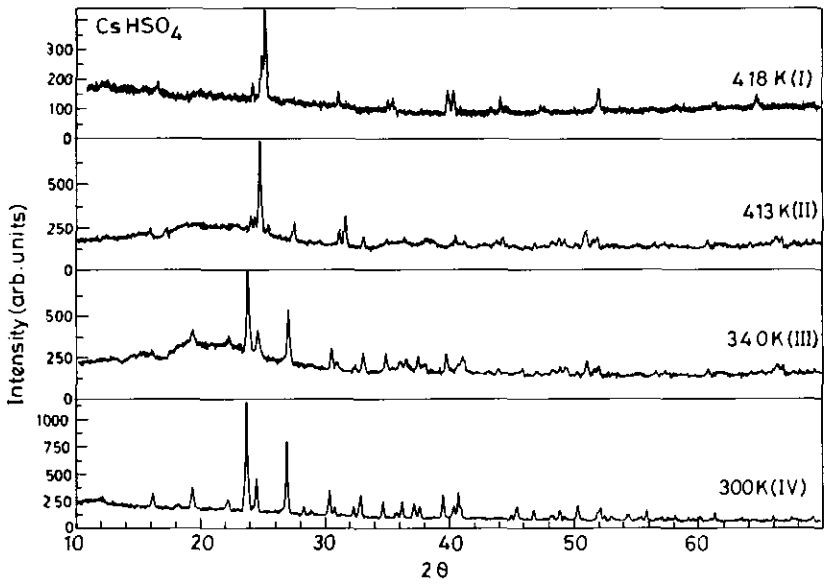

FIG. 8. X-ray diffraction patterns of the different phases of $CsHSO_4$.

TABLE II

UNIT CELL PARAMETERS OF THE DIFFERENT PHASES OF $CsHSO_4$

Phase	T(K)	System	Lattice constants			
			a, Å	b, Å	c, Å	$\beta°$
IV	300	Monoclinic	7.339(001)	5.837(001)	5.517(001)	101.52(01)
II	413	Monoclinic	7.376(008)	11.1426(020)	10.004(011)	97.19(13)
I	418	Tetragonal	5.714(002)	5.714(002)	14.212(006)	—

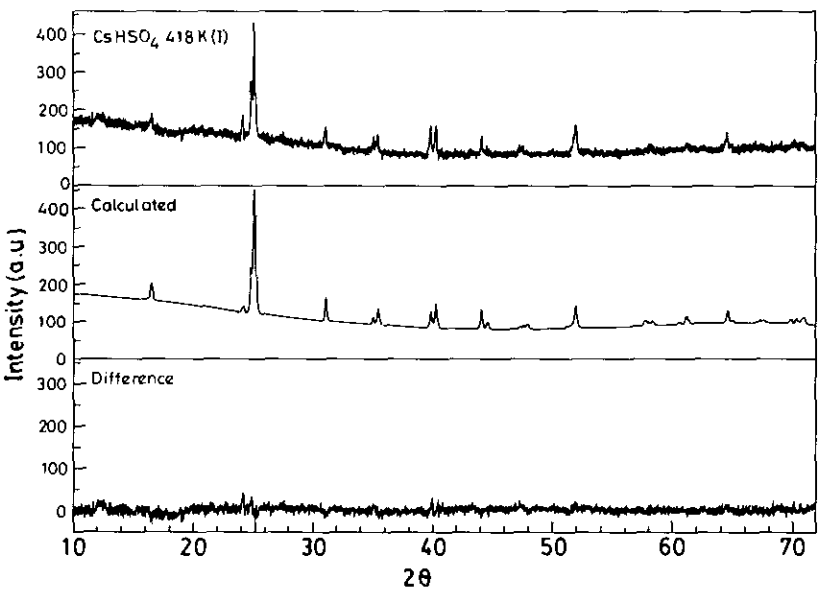

FIG. 9. Observed, calculated, and difference X-ray diffraction patterns of the superionic phase of $CsHSO_4$ (I).

TABLE III

ATOMIC COORDINATES OF $CsHSO_4$(I)[a]

Atom	(Å)			Occ. factor	U (Å^2)
	x	y	z		
Cs	0.5	0.25	0.125	1	0.0048(73)
S	0.0	0.75	0.125	1	0.0161(03)
O	0.2034(01)	0.6553(02)	0.085(01)	0.5	0.0161(03)
*H[b]	0.19	0.5	0.0	0.25	0.03

[a] $R_{(p)} = 0.055$, $R_{(wp)} = 0.071$, $R_{(I,hkl)} = 0.25$.
[b] Hydrogen positional and temperature factors are fixed on the basis of the neutron study (8).

$Cs_{1-x}Li_xHSO_4$

On progressive substitution of cesium by lithium in $CsHSO_4$, the phase transitions disappear (Fig. 1). Infrared spectra of $Cs_{1-x}Li_xHSO_4$ (x = 0–0.3) are shown in Fig. 10. The changes observed on Li substitution are similar to those found on heating $CsHSO_4$ through the phase transitions. Accordingly, on Li substitution the HSO_4^- libration and O · · · O stretching frequencies decrease and the 470 cm^{-1} (S–OH deformation) band disappears; the triplet around 420 cm^{-1} (δSO_4), as well as the bands at 875 cm^{-1} (S–OH stretch) and 1050 cm^{-1} (S–O

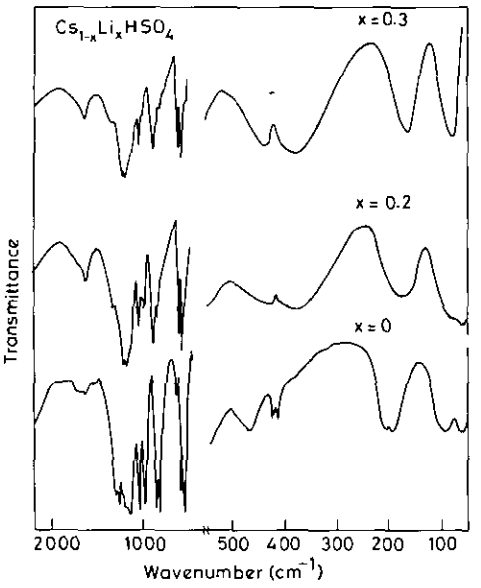

FIG. 10. Infrared spectra of $Cs_{1-x}Li_xHSO_4$.

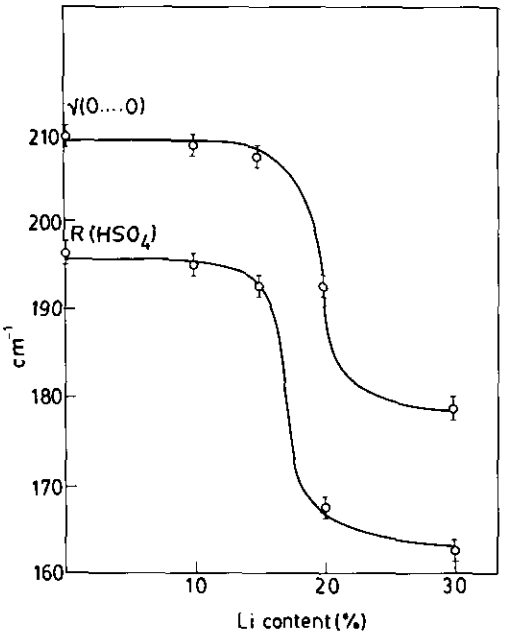

FIG. 11. Variation of the infrared band frequencies due to HSO_4^- libration and O · · · O stretching mode with lithium content.

stretch), loses its structure. In addition, a lithium–oxygen polyhedral mode appears around 380 cm^{-1} as a broad band. In Fig. 11, we show the variation of $RHSO_4^-$ and O · · · O stretching bands with Li content. The $RHSO_4$ band decreases from 196 cm^{-1} in $CsHSO_4$ (x = 0.0) to 167 cm^{-1} when x = 0.3. Rotation of HSO_4^- has been described as a soft mode (*8*) for the superionic transition (II–I). It is interesting that we find softening of this band with respect to temperature as well as lithium substitution.

Raman spectra of $Cs_{1-x}Li_xHSO_4$ (Fig. 12) show a shift in the ν(S–O) band by 25 cm^{-1}. The multiplet around 600 cm^{-1} (ν_4SO_4) loses its structure when x = 0.2. When x = 0.3, the band at 470 cm^{-1} disappears and all the bands become broad. It appears that with increase in lithium substitution disorder increases. Comparing the IR and Raman data of the different phases of $CsHSO_4$ with those of $Cs_{1-x}Li_xHSO_4$, we find that progressive lithium substitution induces the IV–III and III–II transitions. With 30% lithium substitution, the degree of disorder is somewhere between that of phase II and that of the superionic phase I. Further substitution does not seem to have any effect.

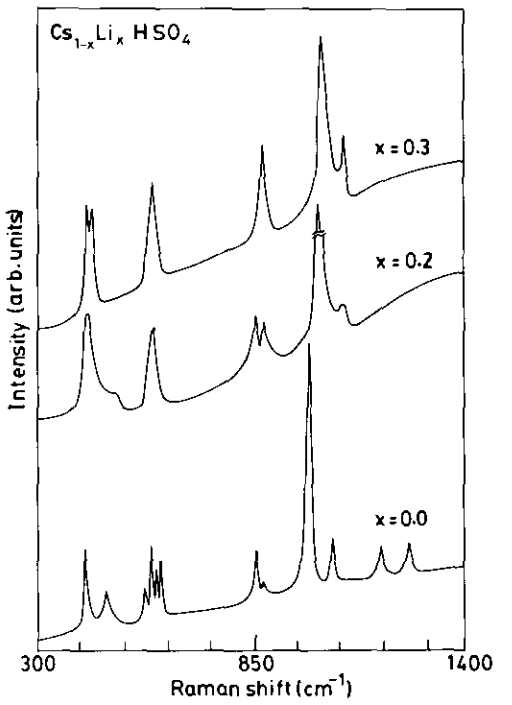

FIG. 12. Raman spectra of $Cs_{1-x}Li_xHSO_4$.

References

1. T. Mhiri, A. Daoud, and Ph. Colomban, *Phase Transitions* **14,** 233 (1989).
2. A. T. Baranov, L. A. Shuvalov, and N. M. Schagina, *JETP Lett.* **36,** 459 (1982).
3. A. Lunden, B. Baranowski, and M. Friesel, *Ferroelectrics* **124,** 103 (1991).
4. M. Pham-Thi, Ph. Colomban, A. Novak, and R. Blinc, *J. Raman Spectrosc.* **18,** 185 (1987).
5. V. I. Dmitriev, M. Klanshek, L. T. Latush, B. Orel, L. M. Rabkin, and N. M. Shchagina, *Sov. Phys. Crystallogr.* **31,** 410 (1986).
6. V. P. Dmitriev, V. V. Loshkarev, L. M. Rabkin, L. A. Shuvalov, and Yu. I. Yuzyuk, *Sov. Phys. Crystallogr.* **31,** 673 (1986).
7. A. M. Balagurov, A. V. Belushkin, I. D. Dutt, I. Natkaniec, N. M. Plakida, B. N. Savenko, L. A. Shuvalov, and J. Wasick, *Ferroelectrics* **63,** 59 (1985).
8. Z. Jirak, M. Dlouha, S. Vrastislav, A. M. Balagurov, A. I. Beskrovnyi, V. I. Gordelii, I. D. Dutt, and L. A. Shuvalov, *Phys. Status Solidi A* **100,** K 117 (1987).
9. M. Pham-Thi, Ph. Colomban, A. Novak, and R. Blinc, *Solid State Commun.* **55,** 265 (1985).
10. B. Baranowski, M. Friesel, and A. Lunden, *Z. Naturforsch.* **419,** 733 (1986).
11. T. Mhiri and Ph. Colomban, *Solid State Ionics* **35,** 99 (1989).
12. K. Itoh, T. Ozaki, and E. Nakamura, *Acta Crystallogr. Sect. B* **37,** 1908 (1981).
13. Ph. Colomban, M. Pham-Thi, and A. Novak, *Solid State Ionics* **24,** 193 (1987).